

Development of High-Pressure Sliding Process for Microstructural Refinement of Rectangular Metallic Sheets

Tadayoshi Fujioka* and Zenji Horita

Department of Materials Science and Engineering, Faculty of Engineering Kyushu University, Fukuoka 819-0395, Japan

A new processing technique, called in this study as high-pressure sliding (HPS), was developed as a process of severe plastic deformation (SPD). It is then demonstrated that HPS can be used for grain refinement of metallic sheets with a rectangular shape which was difficult with a conventional high-pressure torsion utilizing disk samples. Application of HPS to pure Al (99.99%) showed that the grain refinement is achieved with the extent similar to other SPD techniques. [doi:10.2320/matertrans.MRP2008445]

(Received December 4, 2008; Accepted February 3, 2009; Published March 18, 2009)

Keywords: severe plastic deformation, grain refinement, pure aluminum

1. Introduction

It is now well known that significant grain refinement is achieved through application of severe plastic deformation (SPD).^{1,2)} High-pressure torsion (HPT) is a typical SPD process producing ultrafine grains in many metallic materials.^{3–5)} It has an advantage over other SPD processes that the grain refinement is more effective as it is possible to introduce very large strain and it is applicable to rather less ductile materials.^{6–9)} It is also capable of consolidating powders and machining chips without relying on sintering process.^{10–14)} Major limitation of the HPT process is that the sample size is small because it is used in a form of thin disk with typically the size of 10–20 mm in diameter and ~1 mm in thickness. Recent study showed that the HPT process may not be necessarily used with the disk shape but is feasible with samples having a cylindrical bulk form¹⁵⁾ or a ring form.¹⁶⁾ This suggested promising to enhance an opportunity for scaling-up the HPT process. In practice, it was demonstrated that the HPT was successfully attempted with a 100 mm ring with 3 mm width.¹⁷⁾ However, it is desired if the HPT process is used with a form of sheet. In this study, a new SPD process is developed which is applicable for rectangular sheet metallic materials.

2. Principle

As schematically illustrated in Fig. 1, the facility for the new process consists of two anvils and one plunger. The plunger has two grooves on the upper and lower surfaces. Each of the upper and lower U-shape anvil has also a groove on the inner bottom surface. The rectangular sheet samples are then placed on the grooves and a load is applied through the anvils. The plunger is then pushed from one side to the other and shear strain is introduced in the sheet under high pressure. This process is now designated as high-pressure sliding (HPS) for convenience. It is different from HPT such that the HPS no longer requires rotation of the anvils but sliding between the anvils. With the HPS, it is possible to process for rectangular sheets and may provide potential to

scale-up as in the HPT process for rings because equal strain is generated throughout the sample under the same load. The equivalent strain introduced with this process, ε , is given by the form as

$$\varepsilon = \frac{x}{\sqrt{3}t}$$

where x is the sliding length and t is the sample thickness. In this study, the HPS process is applied to pure Al sheets and it is shown that the microstructure and mechanical properties are produced in consistence with other SPD processes such as ECAP (Equal-Channel Angular Pressing), ARB (Accumulative Roll Bonding) and TE (Twist Extrusion) including HPT. It should be noted that although the principle of the HPS allows reciprocal movement of the plunger, one way movement is attempted in this study to check a practical feasibility of the HPS process.

3. Experimental

High purity Al (99.99%) was used in this study since sufficient data were available for ECAP and HPT processes on this purity. The material was received in a form of plate with dimensions of $10 \times 100 \times 200 \text{ mm}^3$. They were cut to sheets with 5 mm width, 100 mm length and 0.8 mm thickness by a wire-cutting electric discharge machine. The thickness of 0.8 mm was selected for direct comparison with HPT results published earlier.¹⁶⁾

The thin sheets were annealed at 773 K for 1 h to produce an average grain size of $\sim 700 \mu\text{m}$. Line marking was made using felt-tip pens at every 10 mm interval on both surfaces at the same location from the edge to check whether the shear were introduced as designated and in a homogeneous way. HPS was conducted at room temperature with an applied load of 25 tons which leads to a pressure of 0.5 GPa. The plunger was pushed with respect to the surrounding anvils for the distance of 5, 10, 15 or 30 mm which produces equivalent strains of 4.1, 8.2, 12.3 or 24.6, respectively. The load variation on the horizontal plunger was measured during operation by continuously recording the oil pressure of the plunger.

*Corresponding author, E-mail: fujioka@zaiko6.zaiko.kyushu-u.ac.jp

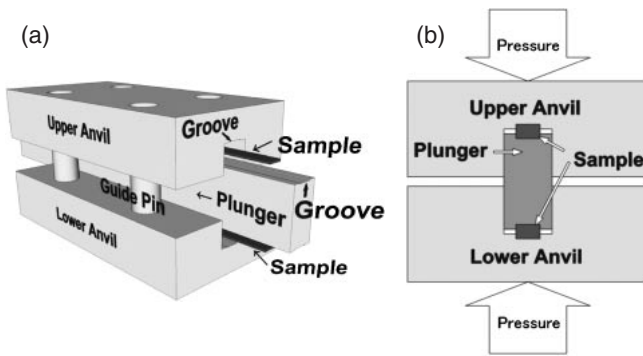


Fig. 1 Schematic illustration of HPS. (a) assembly of two anvils with guiding pins, one plunger and two thin sheet samples. (b) cross sectional view of assembly.

The sheet samples subjected to HPS were polished to a mirror-like surface and thus the Vickers microhardness was measured across the width at 1 mm interval and at every 10 mm along the longitudinal direction over 50 mm length in the center portion of the sheet. For each hardness measurement, a load of 50 g was applied for 15 seconds using an Akashi MVK-E3 testing machine. Tensile specimens with a gauge length of 5 mm and a gauge cross section of $2 \times 0.7 \text{ mm}^2$ were cut from the sheet using a wire-cutting electric discharge machine. The specimens were deformed in tension at room temperature at an initial strain rate of $1.0 \times 10^{-3} \text{ s}^{-1}$.

Transmission electron microscopy (TEM) was conducted on each sample after processing for 5, 10, 15 or 30 mm. Disks with 3 mm in diameter were cut from the sheets and ground mechanically to a thickness of 0.15 mm. They were further thinned with a twin-jet electro-chemical polisher using a solution of 10% HClO_4 , 20% $\text{C}_3\text{H}_8\text{O}_3$ and 70% $\text{C}_2\text{H}_5\text{OH}$ at 273 K. A Hitachi H-8100 transmission electron microscope was operated at 200 kV. Selected area electron diffraction (SAED) patterns were taken to complement the TEM observations using an aperture having a diameter of 6.3 μm .

4. Results and Discussion

Figure 2 shows appearance of a sheet sample after processing by HPS for 30 mm including the sample before HPS. The sample before HPS is shown in Fig. 2(a) and the sample after HPS is shown in Fig. 2(b) for the view from the upper anvil (hereafter designated the UA view or UA surface), Fig. 2(c) for the side view and Fig. 2(d) for the view from the upper side of the plunger (hereafter designated the UP view or UP surface). The line markers made at every 10 mm in the sequence of black, red, green and blue from the left edge of the sample remain at the same positions on the UA surface but those on the UP surface the markers are shifted by 30 mm to the left (the sliding direction) while keeping every marker interval unchanged except both the front and rear edges. This indicates that the shear is equally introduced in the sheet without appreciable slippage and such an equal shear appears over a range of 60 mm. The deviation from the equal shear at the both edges occurs as a consequence of material flows with excess material at the front part and with lack of material at the rear part and for

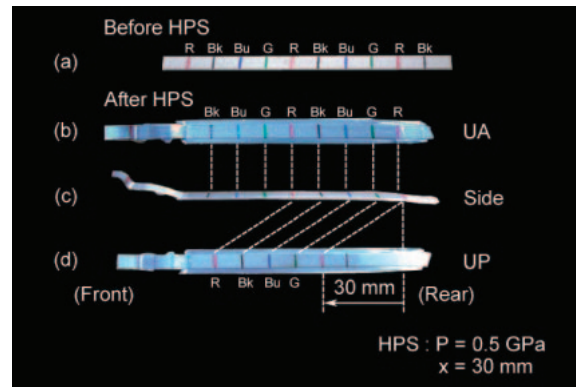


Fig. 2 Appearance of sheet sample (a) before HPS, and after HPS (b) for view from upper anvil (UA surface), (c) for side view and (d) for view from upper side of plunger (UP surface).

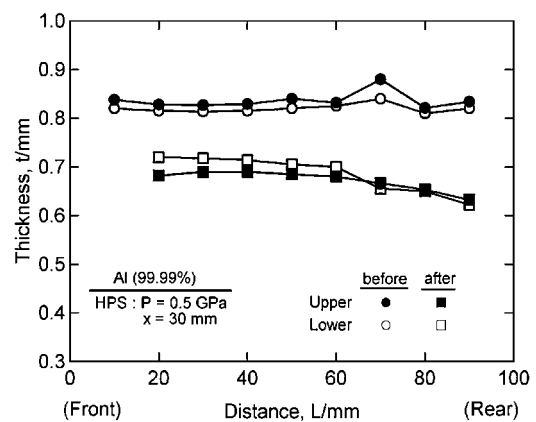


Fig. 3 Thickness variation along longitudinal direction of thin samples before and after HPS for 30 mm.

both parts without applied pressure. It is thus suggested that the longer sample is more efficient for producing regions with equal shear.

Figure 3 plots the thickness variation along the longitudinal direction of the sheet sample before and after processing by HPS. The sliding was given for 30 mm and the thickness measurements were made for the two sheets placed at the upper and lower sides of the plunger. Whereas the thickness is almost equal to ~ 0.83 and ~ 0.81 mm for the upper and lower sheets before HPS, it is reduced to ~ 0.69 mm and ~ 0.71 mm, respectively by HPS and this reduction is consistent with the ones observed in conventional HPT.¹⁸⁾ It should be noted that the thickness reduction near the rear edges becomes prominent and this appears due to the deficiency of material as a consequence of shear near the edge. Such additional decreases in the thickness near the rear edges were also observed even after sliding for 5 mm.

The load variation during pushing the side plunger is shown in Fig. 4. The load increases with time and the side plunger starts to move after ~ 1.5 s (as marked by an arrow) from the moment of the load application. The load further increases with the movement of the side plunger and levels off after ~ 4 s so that the load is kept constant with time at a load level of ~ 15 tons. This load variation is well reproducible until a sudden increase in the load due to the attachment of the plunger on the outer frame holding the

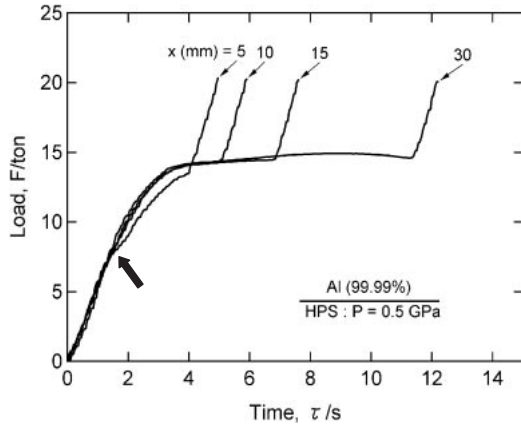


Fig. 4 Load changes with time for sliding distances of 5, 10, 15 and 30 mm. Arrow indicates time for initiation of plunger to move.

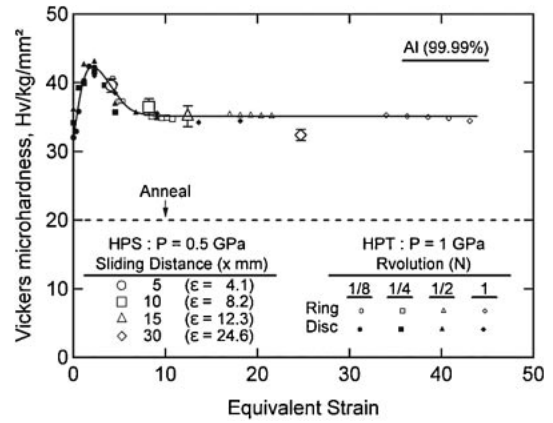


Fig. 6 Vickers microhardness obtained by HPS for sliding distances of 5, 10, 15 and 30 mm. They are plotted against equivalent strain on graph obtained earlier by HPT.¹⁶⁾

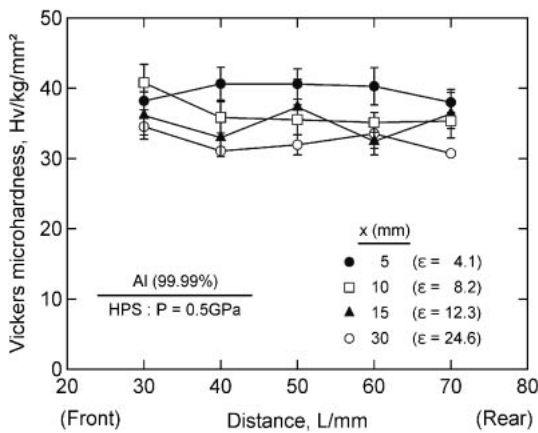


Fig. 5 Vickers microhardness plotted along longitudinal direction of sheet samples for sliding distances of 5, 10, 15 and 30 mm.

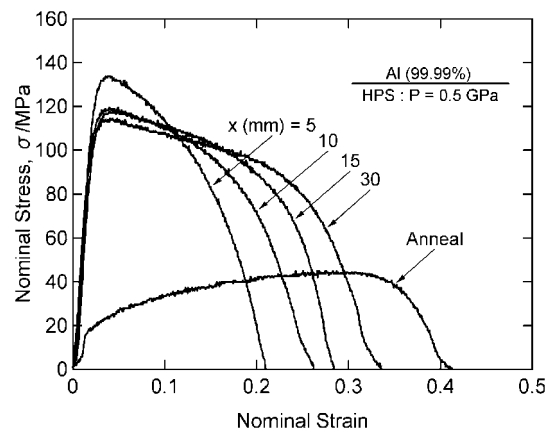


Fig. 7 Nominal stress versus nominal strain for samples processed by HPS for sliding distances of 5, 10, 15 and 30 mm.

anvils. Although the plunger speed was not directly measured in this study, it is estimated from the load variation curves that the plunger moved at a speed of 2.9–3.2 mm/s in average.

Figure 5 plots the hardness measured along the longitudinal direction at every 10 mm of each sample after sliding for 5, 10, 15 and 30 mm. Each point represents the average of 4 measurements made across the sheet width with a 1 mm interval. It appears that the hardness level is highest for the 5 mm sliding and lowest for the 30 mm sliding. The average was taken for each sliding distance and all average values are plotted in Fig. 6 on the earlier figure obtained by HPT.¹⁶⁾ It turns out that the results of both HPS and HPT are very consistent except somewhat lower value obtained by 30 mm sliding with HPS. It is considered that this lower value can be due to a temperature increase during sliding so that softening proceeded to some extent in the HPS-processed Al. The plunger speed, ~3 mm/s, estimated from Fig. 5 corresponds to a rotation speed of more than 6 rpm for a 10 mm disk, which should be high enough for the softening as reported by Todaka *et al.*¹⁹⁾

The stress-strain curves are shown in Fig. 7 after deforming in tension at an initial strain rate of $1 \times 10^{-3} \text{ s}^{-1}$. In consistence with the hardness measurement, the tensile strength is highest for the sample after 5 mm sliding. The strength is reduced to the same level for the other sliding

distances but it is important to note that the total elongation is increased with increasing the sliding distance. The similar trend was reported earlier on the same purity Al although it is less distinctive.²⁰⁾

TEM micrographs of bright and dark field images including selected area electron diffraction patterns are shown in Fig. 8 for the 5 mm and 30 mm processed samples. Dislocations are visible in some grains after processing for 5 mm as indicated by an arrow. There are also areas consisting of grains with ill-defined grain boundaries. For the sample after processing for 30 mm, most of grains are free of dislocations and they are surrounded by well-defined grain boundaries. These microstructural features are consistent with the earlier observations that the dislocation density reaches the highest around the maximum hardness and the portion of the area containing dislocations decreases with further straining before the sample is entirely covered with grains free from dislocations at the steady state. The grain boundary evolution also follows the earlier observations that severe straining of pure Al is accompanied by the formation of well-defined grain boundary with high angle misorientations.

The present study thus demonstrates that the grain refinement is feasible using the process of HPS as other SPD processes such as ECAP, APB and HPT. In particular, the importance of HPS is that this process is usable under the

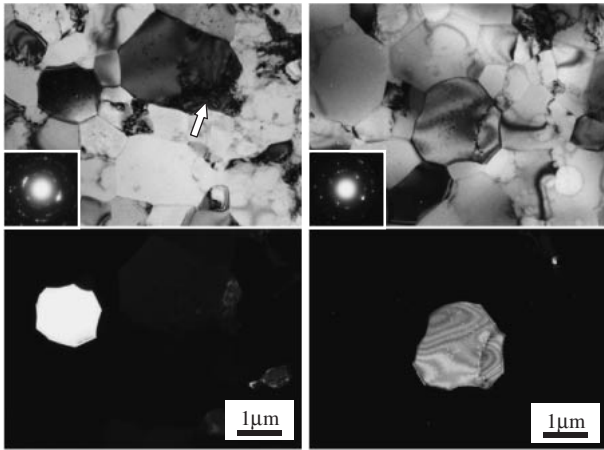


Fig. 8 Bright field images (upper) and dark field images (lower) including SAED patterns.

application of high pressures as in the HPT process and this can permit the processing of less ductile materials for grain refinement and subsequent enhancement of mechanical properties as reported by the studies using HPT. However, it is demonstrated that the HPS process is applicable for materials in a rectangular sheet form.

5. Summary and Conclusions

- (1) HPS was newly developed as an SPD process for grain refinement in rectangular metallic sheets. The HPS facility consists of two anvils and one plunger and each of two sheet samples is placed between the upper anvil and the plunger and the lower anvil and the plunger. The plunger is pushed with respect to the anvils to introduce shear strain in the sheet samples.
- (2) Application of HPS to pure Al (99.99%) led to significant grain refinement with the same hardness level as reported using HPT. It was also shown that the grain size and microstructural features are similar to those produced by HPT.
- (3) It was then demonstrated that HPS can be used as an SPD process for microstructural refinement and subsequent enhancement of mechanical properties under application of high pressure.

Acknowledgements

This work was supported in part by the Light Metals Educational Foundation of Japan, in part by a Grant-in-Aid for Scientific Research from the Ministry of Education, Culture, Sports, Science and Technology of Japan in the Priority Area “Giant Straining Process for Advanced Materials Containing Ultra-High Density Lattice Defects” and in part by Kyushu University Interdisciplinary Programs in Education and Projects in Research Development (P&P).

REFERENCES

- 1) R. Z. Valiev, R. K. Islamgaliev and I. V. Alexandrov: *Prog. Mater. Sci.* **45** (2000) 103–189.
- 2) R. Z. Valiev, Y. Estrin, Z. Horita, T. G. Langdon, M. J. Zehetbauer and Y. T. Zhu: *JOM* **58**(4) (2006) 33.
- 3) A. Vorhauer and R. Pippan: *Scr. Mater.* **51** (2004) 921–925.
- 4) F. Wetscher, A. Vorhauer, R. Stock and R. Pippan: *Mater. Sci. Eng. A* **387–389** (2004) 809–816.
- 5) A. P. Zhilyaev AP and T. G. Langdon: *Prog. Mater. Sci.* **53** (2008) 893–979.
- 6) A. V. Sergueeva, C. Song, R. Z. Valiev and A. K. Mukherejee: *Mater. Sci. Eng. A* **339** (2003) 159–165.
- 7) C. Rentenberger, T. Waitz and H. P. Karnthaler: *Mater. Sci. Eng. A* **462** (2007) 283–288.
- 8) J. Cizek, I. Prochazka, B. Smola, I. Stulíková, R. Kuzel, Z. Matej, V. Cherkaska, R. K. Islamgaliev and O. Kulyasova: *Mater. Sci. Eng. A* **462** (2007) 121–126.
- 9) Y. Harai, M. Kai, K. Kaneko, Z. Horita and T. G. Langdon: *Mater. Trans.* **49** (2008) 76–83.
- 10) I. V. Alexandrov, Y. T. Zhu, T. C. Lowe, R. K. Islamgaliev and R. Z. Valiev: *Nanostruct. Mater.* **10** (1998) 45–54.
- 11) V. V. Stolyarov, Y. T. Zhu, T. C. Lowe, R. K. Islamgaliev and R. Z. Valiev: *Mater. Sci. Eng. A* **282** (2000) 78–85.
- 12) A. R. Yavari, W. J. Botta, C. A. D. Rodrigues, C. Cardoso and R. Z. Valiev: *Scr. Mater.* **46** (2002) 711–716.
- 13) T. Tokunaga, K. Kaneko, K. Sato and Z. Horita: *Scr. Mater.* **58** (2008) 735–738.
- 14) T. Tokunaga, K. Kaneko and Z. Horita: *Mater. Sci. Eng. A* **490** (2008) 300–304.
- 15) G. Sakai, K. Nakamura, Z. Horita and T. G. Langdon: *Mater. Sci. Eng. A* **406** (2005) 268–273.
- 16) Y. Harai, Y. Ito and Z. Horita: *Scr. Mater.* **58** (2008) 469–472.
- 17) K. Edalati and Z. Horita: *Mater. Trans.* **50** (2009) 92–95.
- 18) K. Edalati and Z. Horita: *Mater. Trans.* **50** (2009) 44–50.
- 19) Y. Todaka, M. Umemoto, A. Yamazaki, J. Sasaki and K. Tsuchiya: *Mater. Trans.* **49** (2008) 7–14.
- 20) Z. Horita, K. Kishikawa, K. Kimura, K. Tatsumi and T. G. Langdon: *Mat. Sci. Forum* **558–559** (2007) 1273–1278.